

# Ultrahigh magnetic field phases in the frustrated triangular-lattice magnet $\text{CuCrO}_2$

Atsuhiko Miyata and Oliver Portugall

*Laboratoire National des Champs Magnétiques Intenses, CNRS-UGA-UPS-INSA, 143 Avenue de Rangueil, Toulouse 31400, France*

Daisuke Nakamura, Kenya Ohgushi,<sup>\*</sup> and Shojiro Takeyama<sup>†</sup>

*Institute for Solid State Physics, The University of Tokyo, 5-1-5 Kashiwanoha, Kashiwa, Chiba 277-8581, Japan*

(Received 4 September 2017; published 1 November 2017)

The magnetic phases of a triangular-lattice antiferromagnet  $\text{CuCrO}_2$  were investigated in magnetic fields along the  $c$  axis,  $H \parallel [001]$ , up to 120 T. Faraday rotation and magnetoabsorption spectroscopy were used to unveil the rich physics of magnetic phases. An up-up-down (UUD) magnetic structure phase was observed around 90–105 T at temperatures around 10 K. Additional distinct anomalies adjacent to the UUD phase were uncovered and the Y-shaped and the V-shaped phases are proposed to be viable candidates. These ordered phases emerged as a result of the interplay of geometrical spin frustration, single-ion anisotropy, and thermal fluctuations in an environment of extremely high magnetic fields.

DOI: [10.1103/PhysRevB.96.180401](https://doi.org/10.1103/PhysRevB.96.180401)

In geometrically frustrated magnets, the competition between different magnetic interactions produces highly degenerate magnetic ground states that are vulnerable to tiny perturbations, leading to diverse novel magnetic phases [1]. Among them, one typical state is a multiferroic state in which ferroelectricity is induced by unconventional magnetic structures that arise from geometrical magnetic frustration [2,3]. Since changes in the spin structure alter the ferroelectricity, the application of magnetic fields plays an important role in elucidating the rich variety of magnetic and ferroelectric phases in geometrically frustrated magnet system.

Typical triangular-lattice antiferromagnets that are also multiferroic are  $\text{CuFeO}_2$  [3] and  $\text{CuCrO}_2$  [4,5], both of which are delafossite oxides and have been intensively investigated in the past decade.  $\text{CuFeO}_2$  has a Curie-Weiss temperature of around  $-88$  K and exhibits two successive phase transitions around 14 and 11 K [3]. Below 11 K, its magnetic structure becomes a four-sublattice collinear antiferromagnetic structure. When a magnetic field is applied to this state, a ferroelectric phase appears between  $\sim 7$  and 13 T, which is induced by a proper-screw magnetic structure. This phenomenon is well described by a theoretical model proposed by Arima [6].

Interestingly, additional magnetic phase transitions successively occur at higher magnetic fields in  $\text{CuFeO}_2$ , and magnetization plateaus with values of  $1/5$  and  $1/3$  of the saturation moment have actually been reported [7]. To date, some theoretical models were proposed to explain this rich occurrence of magnetic and ferroelectric phases. For example, a theory proposed by Fishman *et al.* [8] suggested a spin Hamiltonian into which magnetic interactions are incorporated up to the third-nearest neighbors as well as easy-axis single-ion anisotropy. The importance of spin-phonon couplings was suggested by Wang and Vishwanath [9]. However, none of these theories has been able to provide a general explanation of the magnetic and electric properties of multiferroic  $\text{CuFeO}_2$ , which therefore still remains an open issue.

To illuminate the complicated phases in delafossite oxides forming a triangular lattice, it is crucial to reveal the magnetic phases of another delafossite oxide,  $\text{CuCrO}_2$ , which has been known to have a much smaller easy-axis single-ion anisotropy  $D$  with respect to its primary nearest-neighbor interaction  $J_1$ , in contrast to those of  $\text{CuFeO}_2$  [10–13]. For example, their ratio  $D/J_1$  has been estimated by electron spin resonance (ESR) measurements as  $D/J_1 \sim 0.017$  for  $\text{CuCrO}_2$  and much smaller than  $\sim 0.097$  for  $\text{CuFeO}_2$  [12,13].

$\text{CuCrO}_2$  has Curie-Weiss temperatures of  $-211$  K (magnetic field applied perpendicular to the triangular-lattice plane) and  $-203$  K (parallel to the plane), and exhibits two successive phase transitions around 24.2 and 23.6 K [4,5]. Below 23.6 K, its magnetic structure becomes an incommensurate proper-screw magnetic structure, as identified by neutron studies [14], which induces ferroelectricity. This mechanism is described by the theoretical model of Arima [6].

Remarkably, a recent study of  $\text{CuCrO}_2$  under magnetic fields of up to 65 T applied parallel to the [001] axis by Mun *et al.* showed a rich magnetic-field-induced phase diagram including a few ferroelectric phases [15], which are not reproduced by the theoretical model incorporating further-neighbor interactions and easy-axis single-ion anisotropy proposed for  $\text{CuCrO}_2$  by Fishman [16]. Lin *et al.* conducted Monte Carlo calculations with a model including spatially anisotropic nearest-neighbor interactions and easy-axis single-ion anisotropy terms, which showed good agreement with their new results obtained from an experiment performed under higher magnetic fields up to 92 T [17].

As a consequence of their different magnetic interactions and anisotropy, both delafossite compounds  $\text{CuFeO}_2$  and  $\text{CuCrO}_2$  show clearly different magnetic properties at low temperatures. Therefore, unveiling the high magnetic field phases of  $\text{CuCrO}_2$  could provide further insight not only into the rich magnetic and ferroelectric properties of this material but also of delafossite oxides in general.

In this Rapid Communication, we present magneto-optical studies [Faraday rotation (FR) and magneto-optical spectral absorption measurements] of  $\text{CuCrO}_2$  carried out in ultrahigh magnetic fields up to 120 T and at temperatures down to 5 K. We reveal magnetic phases found in  $\text{CuCrO}_2$ , including the

<sup>\*</sup>Present address: Department of Physics, Tohoku University, 980-8578 Miyagi, Japan.

<sup>†</sup>takeyama@issp.u-tokyo.ac.jp

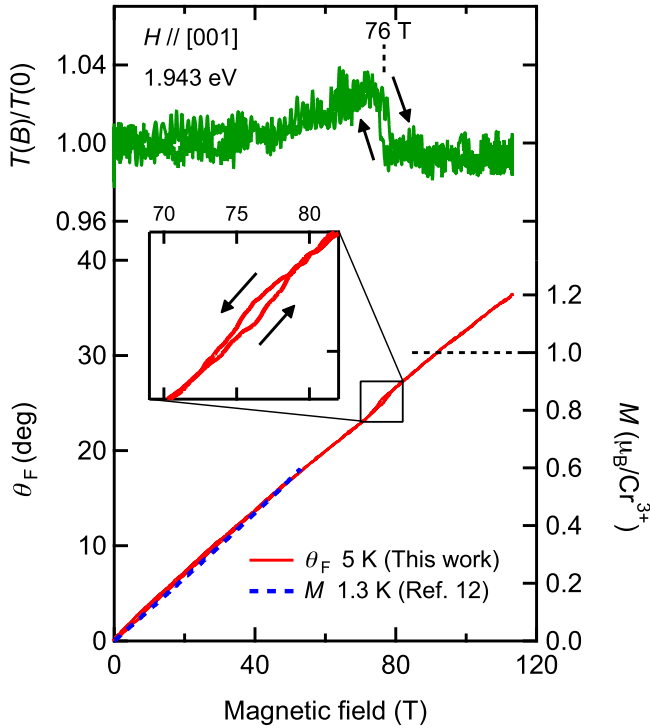


FIG. 1. Normalized magneto-optical transmissions  $T(B)/T(0)$  and Faraday rotation angles  $\theta_F$  obtained by STC at 5 K, together with magnetizations  $M$  obtained at 1.3 K in Ref. [12] ( $H \parallel [001]$ ). Arrows show the hysteresis observed at 76 T.

up-up-down (UUD) magnetic structure phase around 90–105 T at  $\sim 10$  K.

In our experiments a single-turn coil (STC) ultrahigh magnetic field generator (UHMFG) at the Institute for Solid State Physics, University of Tokyo was used to generate magnetic fields exceeding 100 T [18]. Faraday rotation and magneto-optical spectral absorption measurements were conducted up to 120 T using a horizontally aligned STC-UHMFG. The optical alignment around the STC was similar to that described in Refs. [19,20]. Single crystals of  $\text{CuCrO}_2$  were grown by a flux growth method using  $\text{Bi}_2\text{O}_3$  [21]. Platelike samples parallel to the (001) crystal plane about  $10 \times 10 \times 1 \text{ mm}^3$  in size were thus obtained. A sample of  $\text{CuCrO}_2$  with a 2 mm diameter was cut, then polished to a  $50 \mu\text{m}$  thickness, and finally attached to a quartz substrate. The magnetic field was applied parallel to the [001] axis in all measurements. A nonmetallic helium-flow cryostat was used to cool down the sample to temperatures of  $\sim 5$  K [22].

Figure 1 shows the normalized magneto-optical transmission  $T(B)/T(0)$  at a photon energy of 1.943 eV (a wavelength of 638 nm), the Faraday rotation angle  $\theta_F$ , and the corresponding magnetization  $M$ , which is deduced by assuming their proportionality relation  $\theta_F \propto M$ , of  $\text{CuCrO}_2$  under magnetic fields of up to 120 T at 5 K. A magnetization curve obtained by Yamaguchi *et al.* using a nondestructing pulsed magnet up to 50 T at 1.3 K [12] is also shown by a dashed line as a reference in Fig. 1. At 76 T, we observed a clear anomaly associating a hysteresis in both magneto-optical transmissions  $T(B)/T(0)$  and Faraday rotation angles  $\theta_F$ , indicating a first-order phase transition. The anomaly was also

observed in electric polarization measurements performed by Lin *et al.* [17], who suggested that it can be attributed to a phase transition from a commensurate Y-shaped phase (three spins form a Y shape) to the  $1/3$  magnetization plateau (UUD phase). However, according to their Monte Carlo calculations, a transition to the UUD phase cannot be of the first order. In addition, the magnetic moment deduced from the FR angles turned out to be  $\sim 0.83\mu_B/\text{Cr}^{3+}$  at 76 T, which is smaller than what would be expected for the  $1/3$  magnetization plateau ( $1\mu_B/\text{Cr}^{3+}$ ). Therefore, it is natural to regard the phase just above 76 T as another magnetic phase prior to the UUD phase. Details of this phase will be discussed later.

The magnetization deduced from FR angles reaches  $1\mu_B/\text{Cr}^{3+}$  around  $\sim 95$  T, but there is no clear evidence of a plateaulike phase in Fig. 1. The following scenario is the most likely: The  $1/3$  magnetization plateau is known to be caused by an easy-axis anisotropy in classical Heisenberg triangular-lattice antiferromagnets [23]. However, the anisotropy can be released by applying a magnetic field especially above the first-order phase transition at 76 T, which is possibly associated with a lattice distortion. Note that the easy-axis anisotropy of  $\text{CuCrO}_2$  is rather small even in the absence of a magnetic field ( $D/J_1 \sim 0.017$ ) [12]. The reduction of easy-axis anisotropy in magnetic fields has been taken into account, for example, in the sister compound  $\text{CuFeO}_2$ , to explain its magnetic-field-induced phases [7,8].

Even without easy-axis anisotropy, thermal fluctuations can induce the UUD phase in classical Heisenberg triangular-lattice antiferromagnets. This has been studied as the so-called “order by disorder” [23,24]. However, the magnetization appears as an almost linear curve smeared out by temperature as shown in Ref. [24]. This is a viable reason why the  $1/3$  plateau is scarcely observed in current magnetization measurements.

For further investigating details of the magnetic phases in  $\text{CuCrO}_2$ , we conducted magneto-optical transmission spectroscopy (MOTS) of exciton-magnon transitions (EMTs). MOTS of EMTs is sensitive to magnetic phase transitions [25,26] because EMTs occur only when a magnon is required to compensate the spin and angular momentum changes of an otherwise optically forbidden excitonic transition. Spectral structures associated with EMT thus provide strong evidence for a change of both the magnetic and crystal structures. Figure 1 demonstrates that  $T(B)/T(0)$  responds in fact very sensitively to phase transitions.

Figure 2 shows the optical absorption ( $-\log[T(B)]$ ) spectra of the  $d-d$  transition and EMT in  $\text{CuCrO}_2$  measured at 10 K; they are consistent with a previous report by Schmidt *et al.* [27]. The inset shows how the absorption spectrum evolves in magnetic fields up to 100 T in the wavelength region where EMT occurs. The peak intensity of the exciton-magnon absorption first decreases gradually up to 70 T and then increases with a further increase of the magnetic field.

In Fig. 3 the intensity measured at wavelengths between 660 and 680 nm and at temperatures of 7 and 10 K is integrated [integrated absorption intensity (IAI)] and plotted as a function of magnetic field together with the magnetization curve of  $\text{CuCrO}_2$  deduced from the Faraday rotation angles at 5 K. Three distinct anomalies are observed at  $\sim 75$ , 90, and 105 T in IAI (denoted by black triangles in Fig. 3).

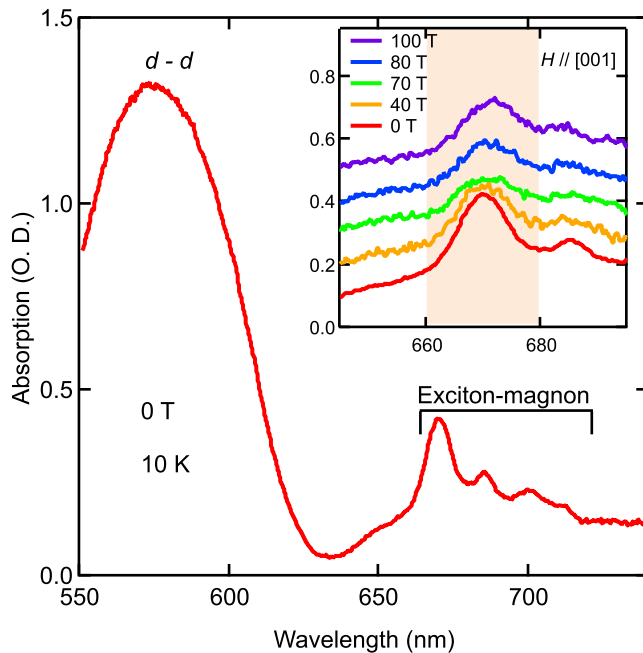


FIG. 2. Optical absorption spectra of  $d-d$  transition and EMT in  $\text{CuCrO}_2$  at 0 T at 10 K. The inset shows magneto-optical absorption spectra in the region of EMTs at several magnetic fields along  $H \parallel [001]$  at 10 K obtained by streak spectroscopy. Absorption peak intensity between 660 and 680 nm is integrated and plotted as a function of magnetic field in Fig. 3.

The anomaly at  $\sim 75$  T corresponds to that observed at 76 T in the magnetization (the corresponding magnetic field differs slightly because of differences in the measurement temperature). A remarkable recovery of IAI is observed above  $\sim 75$  T. In conventional antiferromagnets, the EMT monotonically loses its intensity with increasing magnetic field, since a lesser number of magnons ( $\Delta S_z = +1$ ) compensate for the spin angular momentum during the exciton transition as the spin structure transforms to the canted configuration from the antiparallel configuration under magnetic fields. Magnon creation ( $\Delta S_z = +1$ ) is quenched finally in a fully spin-polarized phase [28].

Therefore, the recovery of the EMT intensity reflects a change of the spin structure above  $\sim 75$  T. The Y-shaped spin structure is the most likely candidate. In this structure, spins approach an antiparallel configuration with increasing magnetic fields, which contributes to an increase of the exciton-magnon absorption intensity. In fact, the increase in the EMT intensity was observed in another multiferroic material,  $\text{BiFeO}_3$ , at the phase transition from the spin spiral to the canted antiferromagnetic phase, which causes an increase in “antiparallelism” [29].

In Fig. 3, around 90–105 T, the EMT intensity goes into a flat-top region (i.e., the maximum of antiparallelism), which indicates that the spins form a collinear up-up-down structure (i.e., UUD phase). The  $1/3$  plateau is scarcely visible in the magnetization ( $M$ ) data. However, the deduced magnetization at 95 T reaches  $1\mu_B/\text{Cr}^{3+}$ , corresponding to the value expected for a  $1/3$  plateau. A slight widening of the flat-topped region is recognized upon increasing temperatures from 7 to 10 K.

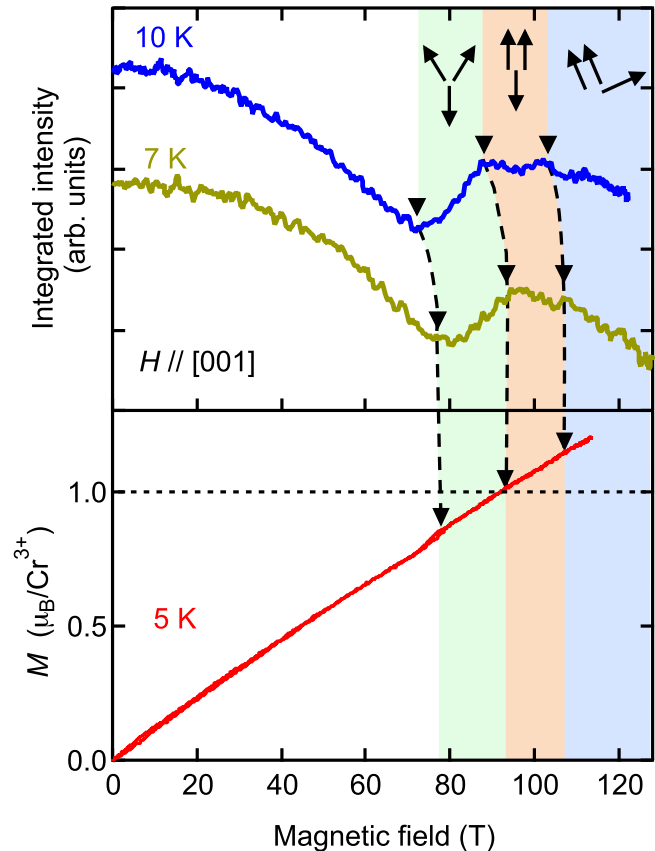


FIG. 3. Integrated absorption intensity in the EMT of  $\text{CuCrO}_2$  at 7 and 10 K at wavelengths between 660 and 680 nm (shaded area in the inset of Fig. 2) and magnetization curve at 5 K deduced from Faraday rotation angles ( $H \parallel [001]$ ). Arrows illustrate spin structures of Y-shaped, UUD, and V-shaped magnetic phases. Dashed lines are a guide to the eyes for phase boundaries.

The UUD phase is known to stabilize by thermal fluctuations [23,24]. Above 105 T, the EMT intensity decreases again. A plausible magnetic phase above the UUD phase is a V-shaped magnetic phase in which two parallel spins and one other spin form a V shape (illustrated by arrows in Fig. 3). V-shaped and Y-shaped magnetic phases have been reported to respectively appear above and below the UUD phase in the phase diagram for a classical Heisenberg antiferromagnet on a triangular lattice with relatively weak easy-axis anisotropy [23].

Figure 4 shows the magnetic phase diagram of  $\text{CuCrO}_2$  up to 120 T. The data for phase transitions in lower magnetic fields refer to measurements of the electric polarization  $P$  ( $H \parallel [001]$  and  $P \parallel [110]$ ) [17] and nuclear magnetic resonance (NMR,  $H \parallel [001]$ ) [30]. Sakhratov *et al.* have assigned regions I and III to a three-dimensionally (3D) ordered incommensurate planar spin-structure phase and a 2D-ordered (or 3D-polar) incommensurate planar spin-structure phase, respectively [30]. Region II is the intermediate phase of I and III with hysteretic behavior. At temperatures below 10 K, the boundary of region “N” was observed in electric polarizations and assigned to an incommensurate umbrellalike spin-structure (cycloidal spiral) phase [17]. Region “C” was attributed to a collinear spin-structure phase that could be connected to the collinear

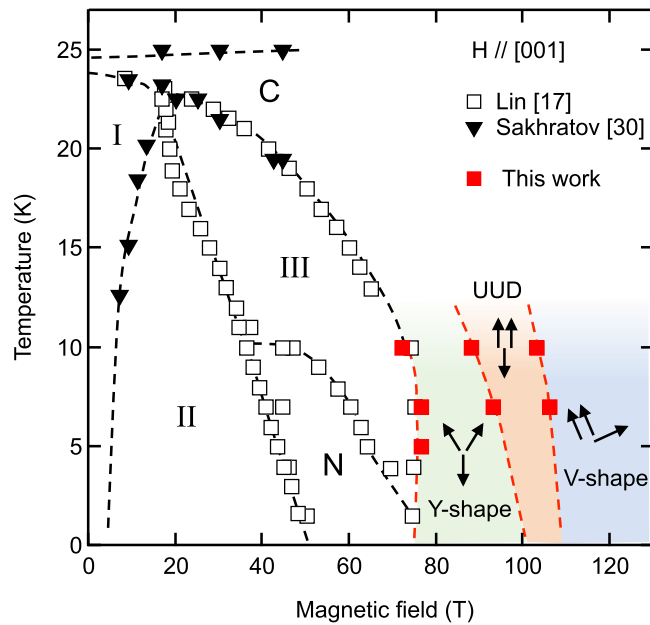


FIG. 4. Magnetic phase diagram of  $\text{CuCrO}_2$  ( $H \parallel [001]$ ). For lower magnetic fields, the data are taken from Refs. [17,30]. Arrows illustrate spin structures of Y-shaped, UUD, and V-shaped magnetic phases. Dashed lines are a guide to the eyes for phase boundaries.

UUD phase that we observed around 90–105 T. The connection between two collinear phases has been theoretically suggested, since thermal fluctuations stabilize the UUD phase even at the zero limit of magnetic field [23]. This behavior has been

observed in magnetic phase diagrams of other triangular-lattice Heisenberg antiferromagnets with easy-axis single-ion anisotropy,  $\text{Rb}_4\text{Mn}(\text{MoO}_4)_3$  [31] and  $\text{Ba}_3\text{MnNb}_2\text{O}_9$  [32].

A striking difference between the magnetic phases of  $\text{CuCrO}_2$  and  $\text{CuFeO}_2$  is that collinear magnetic structures are unstable in  $\text{CuCrO}_2$  in the low-temperature limit. The collinear 1/5 magnetization plateau and collinear four-sublattice antiferromagnetic phase observed in  $\text{CuFeO}_2$  have not been found in  $\text{CuCrO}_2$ . This difference arises from extremely small values of the easy-axis single-ion anisotropy of  $\text{CuCrO}_2$  ( $D/J_1 \sim 0.017$ ) [12], in contrast to that of  $\text{CuFeO}_2$  ( $D/J_1 \sim 0.097$ ) [13].

In summary, magneto-optical measurements of  $\text{CuCrO}_2$  in ultrahigh magnetic fields up to 120 T applied along the [001] axis revealed that the UUD phase exists around 90–105 T at 7–10 K. Furthermore, additional anomalies were observed in the optical absorption intensities of the EMT, which revealed the existence of magnetic phases (presumably the Y-shaped and canted V-shaped phases) below and above the UUD phase. These magnetic phases emerge owing to the interplay of geometrical frustration, the magnetic field, and subtle perturbations of tiny easy-axis single-ion anisotropy and thermal fluctuations.

We acknowledge Masayuki Hagiwara and Hironori Yamaguchi for sending their magnetization data which is shown in Fig. 1, and Kenta Kimura and Masashi Tokunaga for their helpful assistance in growing the samples. A.M. is thankful for the support of the Grant-in-Aid for the Japan Society for the Promotion of Science (JSPS) Fellows.

- [1] *Introduction to Frustrated Magnetism*, edited by C. Lacroix, P. Mendels, and F. Mila, Springer Series in Solid-State Sciences Vol. 164 (Springer, Berlin, 2011).
- [2] T. Kimura, T. Goto, H. Shintani, K. Ishizaka, T. Arima, and Y. Tokura, *Nature (London)* **426**, 55 (2003).
- [3] T. Kimura, J. C. Lashley, and A. P. Ramirez, *Phys. Rev. B* **73**, 220401 (2006).
- [4] S. Seki, Y. Onose, and Y. Tokura, *Phys. Rev. Lett.* **101**, 067204 (2008).
- [5] K. Kimura, H. Nakamura, S. Kimura, M. Hagiwara, and T. Kimura, *Phys. Rev. Lett.* **103**, 107201 (2009).
- [6] T. Arima, *J. Phys. Soc. Jpn.* **76**, 073702 (2007).
- [7] T. T. A. Lummen, C. Strohm, H. Rakoto, and P. H. M. van Loosdrecht, *Phys. Rev. B* **81**, 224420 (2010).
- [8] R. S. Fishman, G. Brown, and J. T. Haraldsen, *Phys. Rev. B* **85**, 020405 (2012).
- [9] F. Wang and A. Vishwanath, *Phys. Rev. Lett.* **100**, 077201 (2008).
- [10] F. Ye, J. A. Fernandez-Baca, R. S. Fishman, Y. Ren, H. J. Kang, Y. Qiu, and T. Kimura, *Phys. Rev. Lett.* **99**, 157201 (2007).
- [11] M. Poienar, F. Damay, C. Martin, J. Robert, and S. Petit, *Phys. Rev. B* **81**, 104411 (2010).
- [12] H. Yamaguchi, S. Ohtomo, S. Kimura, M. Hagiwara, K. Kimura, T. Kimura, T. Okuda, and K. Kindo, *Phys. Rev. B* **81**, 033104 (2010).
- [13] T. Fujita, S. Kimura, T. Kida, T. Kotetsu, and M. Hagiwara, *J. Phys. Soc. Jpn.* **82**, 064712 (2013).
- [14] M. Soda, K. Kimura, T. Kimura, M. Matsuura, and K. Hirota, *J. Phys. Soc. Jpn.* **78**, 124703 (2009).
- [15] E. Mun, M. Frontzek, A. Podlesnyak, G. Ehlers, S. Barilo, S. V. Shiryayev, and V. S. Zapf, *Phys. Rev. B* **89**, 054411 (2014).
- [16] R. S. Fishman, *Phys. Rev. B* **84**, 052405 (2011).
- [17] S.-Z. Lin, K. Barros, E. Mun, J.-W. Kim, M. Frontzek, S. Barilo, S. V. Shiryayev, V. S. Zapf, and C. D. Batista, *Phys. Rev. B* **89**, 220405(R) (2014).
- [18] K. Nakao, F. Herlach, T. Goto, S. Takeyama, T. Sakakibara, and N. Miura, *J. Phys. E* **18**, 1018 (1985).
- [19] A. Miyata, H. Ueda, Y. Ueda, Y. Motome, N. Shannon, K. Penc, and S. Takeyama, *J. Phys. Soc. Jpn.* **80**, 074709 (2011).
- [20] A. Miyata, H. Ueda, Y. Ueda, Y. Motome, N. Shannon, K. Penc, and S. Takeyama, *J. Phys. Soc. Jpn.* **81**, 114701 (2012).
- [21] K. Kimura, H. Nakamura, K. Ohgushi, and T. Kimura, *Phys. Rev. B* **78**, 140401(R) (2008).
- [22] S. Takeyama, M. Kobayashi, A. Matsui, K. Mizuno, and N. Miura, in *High Magnetic Fields in Semiconductor Physics*, edited by G. Landwehr, Springer Series in Solid State Sciences Vol. 71 (Springer, Berlin, 1987), p. 555.
- [23] M. Yun and G. S. Jeon, *J. Phys.: Conf. Ser.* **592**, 012111 (2015).
- [24] H. Kawamura and S. Miyashita, *J. Phys. Soc. Jpn.* **54**, 4530 (1985).
- [25] A. Miyata, S. Takeyama, and H. Ueda, *Phys. Rev. B* **87**, 214424 (2013).
- [26] A. Miyata, H. Ueda, Y. Ueda, H. Sawabe, and S. Takeyama, *Phys. Rev. Lett.* **107**, 207203 (2011).

- [27] M. Schmidt, Z. Wang, Ch. Kant, F. Mayr, S. Toth, A. T. M. N. Islam, B. Lake, V. Tsurkan, A. Loidl, and J. Deisenhofer, *Phys. Rev. B* **87**, 224424 (2013)
- [28] V. V. Eremenko, Yu. G. Litvinenko, and V. V. Shapiro, *Fiz. Nizk. Temp.* **1**, 1077 (1975) [*Sov. J. Low Temp. Phys.* **1**, 519 (1975)].
- [29] X. S. Xu, T. V. Brinzari, S. Lee, Y. H. Chu, L. W. Martin, A. Kumar, S. McGill, R. C. Rai, R. Ramesh, V. Gopalan, S. W. Cheong, and J. L. Musfeldt, *Phys. Rev. B* **79**, 134425 (2009).
- [30] Yu. A. Sakhratov, L. E. Svistov, P. L. Kuhns, H. D. Zhou, and A. P. Reyes, *Phys. Rev. B* **94**, 094410 (2016).
- [31] R. Ishii, S. Tanaka, K. Onuma, Y. Nambu, M. Tokunaga, T. Sakakibara, N. Kawashima, Y. Maeno, C. Broholm, D. P. Gautreaux, J. Y. Chan, and S. Nakatsuji, *Europhys. Lett.* **94**, 17001 (2011).
- [32] M. Lee, E. S. Choi, X. Huang, J. Ma, C. R. Dela Cruz, M. Matsuda, W. Tian, Z. L. Dun, S. Dong, and H. D. Zhou, *Phys. Rev. B* **90**, 224402 (2014).